Laser-light scattering, a new method for continuous monitoring of platelet activation in circulating fluid

GEORGE S. ABELA, RUIPING HUANG, HONGBAO MA, ALEJANDRO R. PRIETO, MING LEI, ALVIN H. SCHMAIER, KENNETH A. SCHWARTZ, and JOHN M. DAVIS

EAST LANSING and ANN ARBOR, MICHIGAN

We evaluated a novel technique of laser-light scattering (LLS) to detect platelet-volume changes continuously, reflecting platelet aggregation in circulating fluid. Carotid arteries from 20 dogs were mounted in a dual perfusion chamber. Balloon angioplasty (BA) was performed and arteries perfused with platelet-rich plasma (PRP). A He-Ne laser beam was passed through cuvettes connected to tubing draining the arteries. From the angle of incidence, the average volume of aggregates was measured by the ratio of scattering light at 1 to 5 degrees' spread on the diode array of a multichannel analyzer. Platelet volume varied linearly with the scattered light ratio at 1 to 5 degrees ($y = -24.2 + 27.6\ x$ (y = particle size, μm^3; x = scattered light ratio at 1/5 degrees)). For comparison, we used an electronic particle counter (Coulter counter) to measure platelet volume. *P*-selectin expression was measured to confirm platelet activation. Comparing 10 uninjured and 10 BA-injured arteries, we found that platelet volume as measured with LLS increased from 21.6 ± 4.1 to $52.1 \pm 12.5\ \mu m^3$ ($P < .003$); as measured with the Coulter counter, it increased from 29.9 ± 2.4 to $62.3 \pm 7.0\ \mu m^3$ ($P < .005$). Six BA-injured arteries perfused with PRP and aspirin (0.2 mg/mL) were compared with six arteries treated with BA alone. The aspirin decreased platelet volume as measured with LLS from 56.2 ± 11.8 to $40.2 \pm 12.7\ \mu m^3$ ($P < .01$); the Coulter counter revealed a decrease from 51.9 ± 18.5 to $38.8 \pm 14.2\ \mu m^3$ ($P < .001$). Coulter counter and LLS results were correlated: $r = 0.74$, $P < .05$. The peak of *P*-selectin expression coincided with peak platelet volume. These data demonstrate that increases in circulating-platelet size stimulated by endovascular injury can be reliably and continuously monitored with the use of LLS. (J Lab Clin Med 2003;141:50-7)

Abbreviations: BA = balloon angioplasty; LLS = laser-light scattering; NHSF = *N*-hydroxysuccinamide fluorescein; PBS = phosphate-buffered saline solution; PRP = platelet-rich plasma; RBC = red blood cell; SEM = scanning electron microscopy

Application of the laser-light scattering (LLS) technique in the measurement of platelet aggregation was first proposed by Hubbell et al in their seminal work of 1991.[1] Compared with the conventional aggregometer, this technique has the advantage of being a more sensitive method for the detection of microaggregates (two or three platelets) and has the ability to measure the rate of formation of

From the Divisions of Cardiology, Hematology-Oncology, and Physics, Department of Medicine, Michigan State University; and the Division of Hematology-Oncology, Department of Internal Medicine, University of Michigan.

Supported in part by grants from the National Institutes of Health (SBIR phase 1 [HL55907 as a subcontract from Thromgen, Inc]) and an A. W. Ford Memorial Institute Grant.

Submitted for publication February 27, 2002; revision submitted September 3, 2002; accepted September 24, 2002.

Reprint requests: George S. Abela, MSc, MBA, MD, Michigan State University, Department of Medicine/Cardiology, B-208 Clinical Center, East Lansing, MI 48824; e-mail: george.abela@ht.msu.edu.

0022-2143/2003 $30.00 + 0

doi:10.1067/mlc.2003.4

platelet aggregates in real time.[2] Several cardiovascular applications of this concept have since been successfully performed, including the detection of small platelet aggregates during cardiopulmonary bypass and in acute coronary syndromes.[3] However, in these studies, platelet aggregates were measured after peripheral-blood samples were obtained from patients.[4] We hypothesize that the LLS technique could be adapted for continuous measurements of the volume of circulating individual platelets and used to monitor changes in platelet volume that occur with platelet activation and subsequent aggregation. LLS could be a practical means of studying inhibition or induction of platelet aggregation in the evaluation of the effects of various antiplatelet agents.

In this study, we evaluated the ability of the LLS technique to continuously detect platelet aggregate formation after arterial balloon-induced injury in canine arteries and correlated this with the well-established Coulter-counter method. As an example, we used the LLS technique and the Coulter-counter method to measure aspirin-induced inhibition of platelet aggregation stimulated by balloon injury to the arterial intima. Results from the LLS technique were highly correlated with those from the Coulter-counter method, and LLS had the advantage of providing continuous measurement of platelet aggregation in real time.

METHODS

Dogs. In this study, 20 male dogs (8 mongrels and 12 beagles, 18-20 pounds) were used. While each dog was under general anesthesia (sodium pentobarbital 65 mg/mL, 0.5 mL/kg IV), whole blood (450 mL) was collected in 50 mL sodium citrate (150 mmol/L). We obtained PRP by centrifuging whole blood at 150*g* in a swing-bucket rotor for 20 minutes at 22°C. The dog was then killed with a lethal-dose euthanasia solution, given intravenously. Dogs were housed in accordance with National Institutes of Health guidelines, and the study was conducted in accordance with the protocol approved by the Michigan State University Animal Care and Use Committee.

Preparation of the carotid artery and BA. Both carotid arteries from each dog were carefully isolated, and all arterial branches were ligated with 4.0 silk suture. Two 5-cm carotid-artery segments from each dog were mounted side by side in a dual perfusion chamber immersed in oxygenated PBSat 37°C (Fig 1). The circulatory setup consisted of silicon tubing (3-mm internal diameter) connected to and emerging from a plastic box with two parallel chambers separated by a plastic divider. A roller pump was used to propel the fluid through the closed circuit at a rate of 70 mL/min. We injured the intimal surface of the carotid-artery segments with the use of a balloon catheter (3 × 30 mm) inflated to 10 atm at three different sites each for 1 minute, starting most distally and moving proximally to avoid overlapping injury. During balloon inflation, we wrapped surgical umbilical tape around the artery at the center of the balloon to create a resistance between the balloon and the arterial wall to ensure vascular injury. The total volume of PRP circulated in each chamber was 60 mL. Platelet concentration in the PRP averaged 5×10^7/mL. The exterior of the arteries was bathed in oxygenated PBS. Both the bathing solution and the circuit were kept at 37°C.

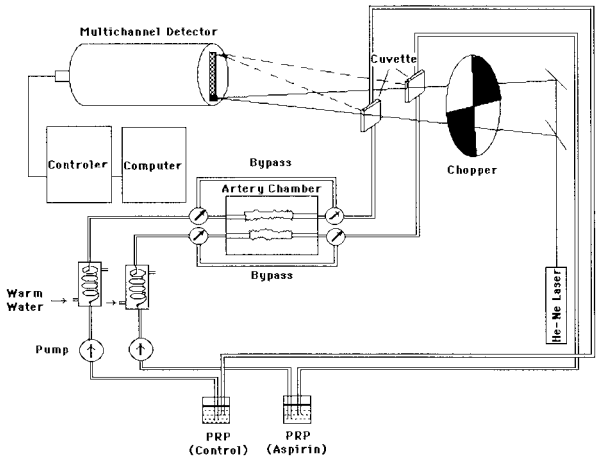

Fig 1. Diagram of the experimental setup, demonstrating the flow of PRP in the arteries of the dual organ chamber. The He-Ne laser beam was split by a beam chopper to enter the cuvettes and displayed the LLS on the diode array at 1 and 5 degrees.

Three groups were evaluated. Group 1 comprised 20 arteries: 10 uninjured arteries and 10 BA-injured arteries perfused with PRP. Group 2 included 12 arteries: 6 BA-injured arteries perfused with PRP but not treated with aspirin and 6 BA-injured arteries perfused with PRP and treated with aspirin (0.2 mg/mL). Group 3 comprised 8 arteries: 4 BA-injured and 4 uninjured, perfused with PRP in an attempt to evaluate *P*-selectin expression. Total perfusion time for each artery was 60 minutes.

Measurement of platelet volume with the LLS and Coulter-counter methods. A He-Ne laser beam (633 nm) was split and passed through two cuvettes interposed in the tubes draining the two carotid-artery segments. The scattering light from particles in the cuvettes was spread on the diode array of a multichannel analyzer (model ST-120; Princeton Instruments Inc, Princeton, NJ). From the angle of incidence, the ratio of scattering light at 1 to 5 degrees represented particle-size distribution. Small particles have a higher distribution of scattered laser light at the wider angle (5 degrees), whereas large particles have a greater distribution of scattered light at the narrower angle (1 degree).[1] We digitized the electronic signals from the multichannel analyzer using a custom software package, after which we displayed the data graphically on a computer screen and recorded them on a HP Color Pro printer (HP Corp, Palo Alto, Calif) (Fig 1). We carried out measurement of platelet-particle volume as an index of aggregation with the Coulter counter (models Zf and MHR; Coulter Electronics, Inc, Hialeah, Fla) by obtaining 50-μL samples of PRP effluent at 5- to 10-minute intervals during PRP perfusion. We calibrated the counter with parti-

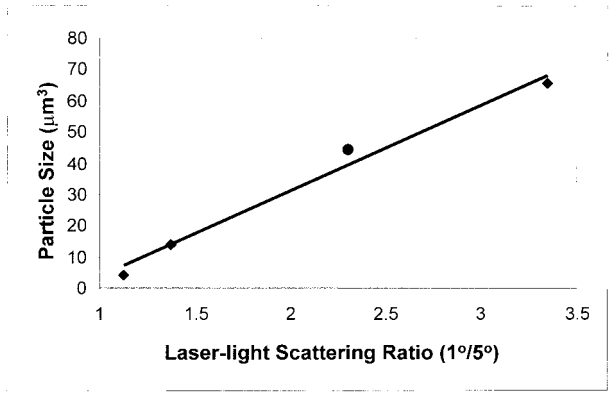

Fig 2. Graph of callibration for LLS using standard particle sizes. The relationship was a linear function represented by $y = -24.2 + 27.6x$, where y is particle size (cubic millimeters) and x is the scattered-light ratio at 1 and 5 degrees. The third point on the graph (●) represents the size of a dog RBC.

cle-size latex beads (2, 3, and 5 μm in diameter; Coulter Electronics). Calibration for the LLS method was carried out with the same size latex beads, as well as canine RBCs (4.4 μm in diameter as determined with the Coulter counter). LLS data were converted from the reflected light angle ratio measurement at 1 and 5 degrees to a volumetric scale involving a standard curve. This curve was generated from LLS of both the latex-particle standards and the dog RBCs of known size (Fig 2).

To evaluate the effect of RBCs on the scattered light signal of the PRP, we conducted optical measurements on PRP alone and with various numbers of RBCs before and after adding ADP to aggregate the platelets. This allowed us to determine what concentration of RBCs in the fluid would mask the ability of the system to detect platelet aggregates. The concentrations of RBCs added ranged from 1×10^5 to 10^8/mL; the PRP concentration was 1×10^8/mL platelets.

Flow cytometric analysis of *P*-selectin expression. We confirmed platelet activation after vascular injury by measuring the expression of canine platelet *P*-selectin. Because *P*-selectin (CD62) is expressed on the surface of activated platelets only, we assessed *P*-selectin expression on platelets used to perfuse BA-injured and uninjured arteries. Detection of canine *P*-selectin was performed with a fluorescein-labeled mouse monoclonal antibody, MDP-1, provided by Dr. Samuel Burstein (University of Oklahoma, Oklahoma City, Okla). We labeled the antibody with fluorescein using NHSF (Pierce Chemical Co, Rockville, Ill). In brief, NHSF was dissolved in dimethylsulfoxide (1 mg/mL) and added in 20-fold molar excess to 1 mg of MDP-1 and allowed to react on ice for 2 hours. We removed unreacted NHSF by diluting the reaction solution with PBS and conducting ultrafiltration through a Centricon-10 ultrafiltration device (Amicon Inc, Beverly, Mass). Test platelets (100 μl) were labeled with 10 μg of fluorescein-conjugated MDP-1 for 20 minutes at room temperature. The labeled platelets were then diluted with PBS containing 0.025% NaN_3 and incubated at room temperature until they could be analyzed. Flow-cytometric study was performed with a Vantage flow cytometer (Becton-Dickinson Co, San Jose, Calif). Excitation was carried out at 488 nm, detection at 530 nm. We analyzed data with Cell Quest software (Becton-Dickinson). All samples were analyzed 2 to 3 hours after collection.

Histologic examination. We evaluated thrombogenicity of treated sites by examining perfusion-fixed arterial segments under light microscopy and SEM. Samples for SEM were taken from each of the arterial segments after 1 hour's perfusion, then subjected to critical-point drying in liquid carbon dioxide, mounted on stubs, and gold-coated in a sputter coater. The SEM of the intimal surface was examined with a JEOL scanning electron microscope (model JSM-6400V; JEOL Ltd, Tokyo, Japan), and representative sections were photographed. The other arterial homografts were embedded in paraffin and mounted on glass slides. Fixed, paraffin-embedded tissues were cut into 7-μm-thick sections and stained with hematoxylin and eosin and Masson's trichrome, after which they were examined with a light microscope.

Statistical analysis. Data are reported as mean ± SD and were compared with the use of paired Student *t* tests. We considered *P* values of less than .05 statistically significant. SigmaStat statistical software was used to calculate statistical comparison (Sigma, St. Louis, Mo). We conducted a correlation analysis of the platelet-volume measurements obtained with the use of LLS and with the Coulter counter.

RESULTS

The measurements obtained with LLS were dependent on the ratio of scattered light at 1 and 5 degrees. The ratio of 1 to 5 degrees increased with increasing particle size, as shown in the standard curve derived from the measurements of four known particle sizes (Fig 2). Platelet volume was calculated from the scattered-light ratio of 1 to 5 degrees as determined with the following equation: $y = -24.2 + 27.6\ x$, where y is particle size as an indirect measurement of platelet volume (cubic micrometer) and x is the scattered-light ratio at 1 and 5 degrees. Non-activated platelets are discoid and measure approximately 2 μm in diameter, with a volume of about 5 μm^3. Because our measurement of platelet volume was 20 to 60 μm^3, these data reflect measurements of platelet aggregates.

PRP volume measurements, alone and with RBCs, demonstrated no significant masking of the scattered-light pattern before and after aggregation with ADP at RBC concentrations of up to 6×10^6/mL (Fig 3). The pattern was partially masked at 1×10^7/mL and obliterated by 1×10^8/mL.

Platelet-volume measurements obtained with the use of LLS were compared with those obtained with the Coulter counter in groups 1 and 2. In group 1, platelets exposed to BA-injured arteries demonstrated a significant increase in volume, which we considered to represent platelet activation and formation of platelet aggregates. In group 2, inhibition of platelet activation

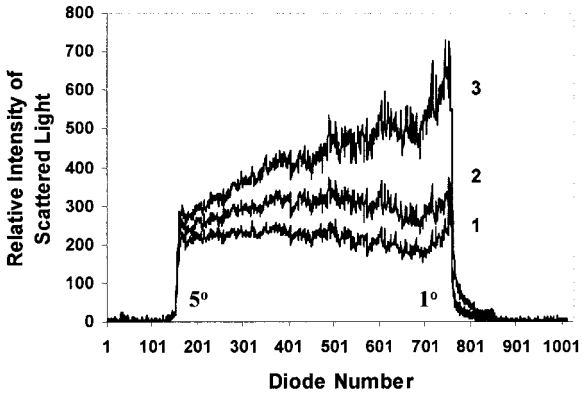

Fig 3. Graph of three light-scattering patterns: **(1)** PRP at 1.2×10^8; **(2)** PRP with RBCs at 2×10^6; **(3)** PRP and RBCs after the addition of ADP to induce platelet aggregation. Graph 2 does not mask graph 3, and the platelet-aggregate scattering pattern is not blocked.

with aspirin significantly reduced the increase in platelet volume (Fig 4). These measurements were reported at the peak change in platelet volume that occurred 15 minutes after the initiation of PRP circulation. Also, the comparisons of LLS and Coulter-counter measurements for groups 1 and 2 reported in Figs 5 and 6 were made at the same peak effect.

In group 1, 20 arteries were studied: 10 uninjured controls and 10 with BA-induced injury. The platelet volume measured with LLS increased from a control of 21.6 ± 4.1 to $52.1 \pm 12.5 \mu m^3$ after injury ($P < .005$). Platelet volume as measured with the Coulter counter increased from a control value of 29.9 ± 2.4 to $62.3 \pm 7.0 \mu m^3$ after injury ($P < .003$; Fig 5).

In group 2, 12 BA-injured arteries were studied: 6 perfused with PRP but not treated with aspirin and 6 treated with aspirin. Aspirin treatment decreased platelet volume, a finding detected both with LLS and with the Coulter counter. Platelet volume as measured with LLS decreased from a control of 56.2 ± 11.8 to 40.2 ± 12.7 μm^3 with aspirin ($P < .01$). Platelet volume as measured with the Coulter counter decreased from a control of 51.9 ± 18.5 to 38.8 ± 4.2 μm^3 with aspirin ($P < .01$; Fig 6).

Comparison of findings obtained with the LLS and Coulter counter methods showed a high correlation ($r = .74$, $P < .05$). These data suggest that the LLS method can be used to provide real-time continuous measurement of platelet-aggregate size in the circulation after vascular injury.

To determine whether platelet volume was reflective of platelet activation, we sampled platelets after circulation in 8 arteries (group 3; 4 injured and 4 uninjured) and measured platelet volume with the Coulter counter and LLS. Using the monoclonal antibody MDP-1, we found that the percent expression of *P*-selectin in the

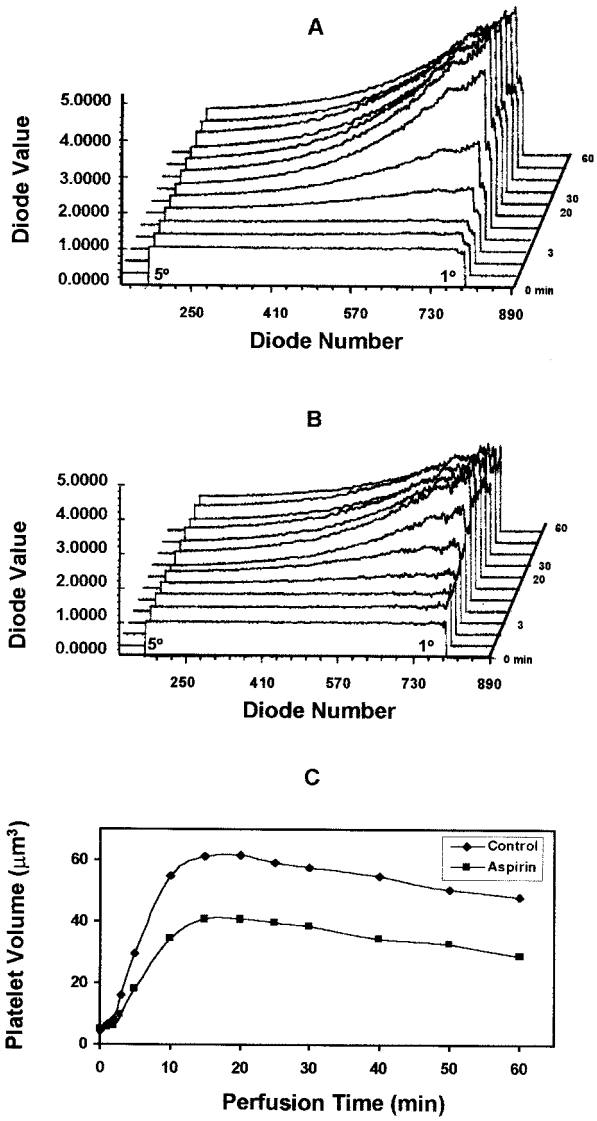

Fig 4. **A**, Laser-light scattering distribution at 1 and 5 degrees, emitted from the circulating PRP effluent in a BA-injured artery. **B**, LLS distribution at 1 and 5 degrees, emitted from the circulating PRP effluent in a BA-injured artery exposed to aspirin. **C**, Cumulative platelet volume over 60 minutes from LLS data collected in *A* and *B*.

PRP used to perfuse the arteries was consistently higher at 15 minutes than at the immediate baseline (Fig 7). These data demonstrate simultaneous platelet activation with increased LLS, suggesting that platelets were activated as they traversed the circuit.

Light microscopy of BA-treated arterial segments showed medial dissection and stretching of the arterial wall. These injuries were prominent at sites where umbilical tape was used to create resistance to balloon inflation. Also, platelet aggregates were seen attached to sites of disrupted endothelium (illustration not shown).

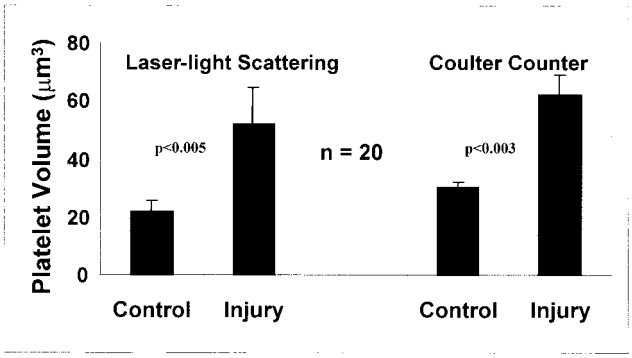

Fig 5. Bar graphs of platelet-volume measurements comparing the LLS and Coulter-counter methods in normal and BA-injured arteries. BA injury significantly increased platelet-aggregate volume compared with that in control uninjured arteries with both methods. These measurements were obtained at the peak effects, seen at 15 minutes.

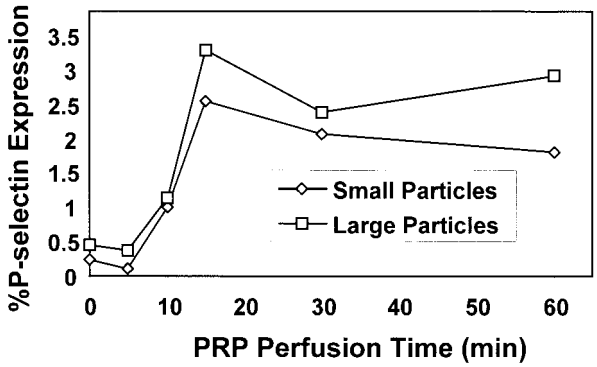

Fig 7. Percent *P*-selectin expression and perfusion time. This is an example of one study demonstrating peak *P*-selectin expression at 15 minutes for both small and large particles. This is coincident with the time for aggregate peak detected both with LLS and the Coulter counter in *Figs 3* through *6*.

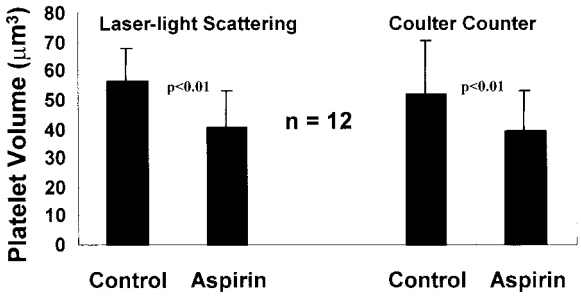

Fig 6. Bar graphs of platelet-volume measurements taken with the LLS and Coulter-counter methods in BA-injured arteries with and without aspirin. Aspirin significantly decreased platelet-aggregate volume compared with that seen in the control injured arteries. These measurements were obtained at the peak effects, seen at 15 minutes.

SEM examination of the BA-treated arterial segments showed wedge-shaped intimal-surface tears. Extensive platelet adhesion was noted to cover the arterial surface at sites of intimal injury. Arteries perfused with PRP and treated with aspirin demonstrated less platelet adhesion compared with BA-injured controls (Fig 8). Normal control arterial segments showed an intact endothelial surface demonstrating a typical cobblestone appearance without platelets (illustration not shown).

DISCUSSION

The LLS device actually reports changes in platelet volume that occur after exposure to vascular injury in an in vitro circuit. We have already used this method to evaluate a new antiplatelet agent, thrombostatin.[5] At this time, the utility of this model lies in the continuous evaluation of the effect of potential antiplatelet agents.

Platelet aggregation is conventionally evaluated on the basis of optical-density or electrical-impedance change after the administration of a platelet agonist such as ADP.[6-9] These methods do not provide information about temporal changes in the number or size of platelet aggregates after activation. The LLS technique holds the potential of evaluating platelet inhibition after drug treatment, as well as monitoring platelet activation after interventional procedures.[10] The ability to measure platelet-aggregate formation continuously, without the need for sample collection, is a unique advantage. This allows an investigator to examine various profiles of platelet aggregates as they form over time and to measure the time-dose relationship of inhibition of aggregate production for different inhibitors of platelet function. Unlike the Coulter-counter method, it has the advantage of detecting smaller platelet aggregates and can be used to continuously monitor platelet-aggregate formation in flowing fluid in real time.

The Coulter-counter system relies on the reduction in fluid turbulence as platelets aggregate to form larger particles, allowing more light to be transmitted through the fluid medium. The LLS method relies on the actual particle size, with laser light bouncing off at a greater angle from the surface of the smaller spherical particles, which have a greater curvature. The larger particles reflect light at a lesser angle. Therefore higher resolution might be expected with the LLS method, as has been suggested by Eto et al,[2] who demonstrated that LLS is capable of detecting aggregate particles as small as two platelets. It has been previously established that the LLS technique is more sensitive than conventional aggregometry based on light transmission, and this finding has been confirmed with electronic particle counting and sizing of fixed samples.[1,7] We chose the Coulter method to evaluate platelet-aggregate volume, not the ability of the platelets to

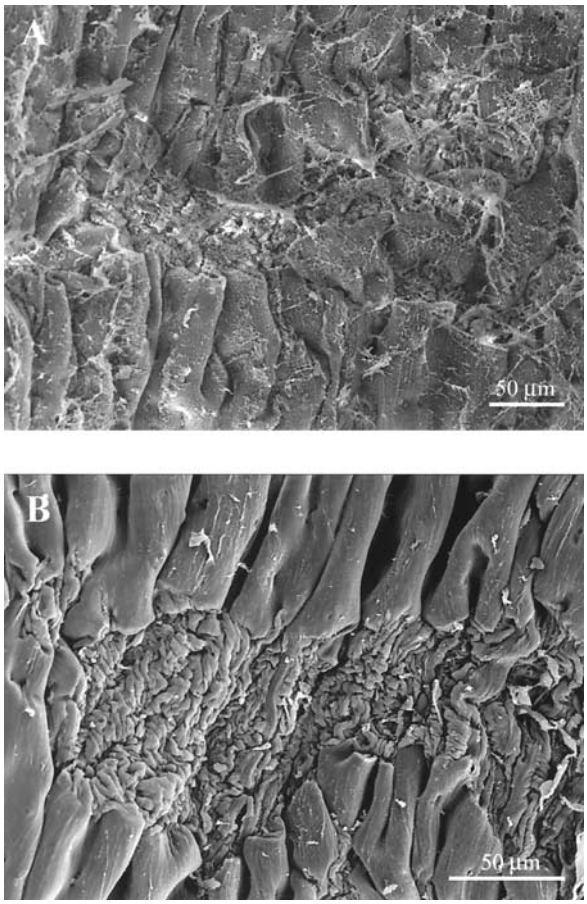

Fig 8. SEM of canine carotid arteries collected after 60 minutes' perfusion with PRP. **A**, SEM of BA-injury site, demonstrating damage to the endothelial lining with some platelet aggregates and scattered fibrin deposition. **B**, Micrograph of BA-injury site of an artery perfused with PRP and aspirin. The endothelial lining was disrupted, and only an occasional platelet was noted.

aggregate, as would be evaluated with standard aggregometry methods. The LLS technique was used to measure platelet volume in continuously circulating PRP, as demonstrated in Fig 1. The measurements obtained with the Coulter-counter technique, on the other hand, were performed after the collection of samples at specific intervals; this may lead to greater variability as a result of sample collection and handling. At the time of this writing, the LLS technique is the only developed method of continuously measuring platelet volume in circulating fluid in an in vitro setup.

P-selectin expression on the circulating platelets successfully demonstrated that the LLS technique and the change in platelet volume were indicative of platelet activation. No significant difference in the amount of *P*-selectin expression was demonstrated between injured and uninjured arterial segments. These findings are consistent with previous reports indicating that *P*-selectin is a variable marker of injury after BA.[11-13] Also, in a previous study we demonstrated a high correlation between radioactivity count from indium 111–labeled platelets and platelet-aggregation measurements taken with LLS.[5] In that study, platelet aggregation in arterial injury alone was significantly greater than that seen in noninjury. Histologic study showed more platelet deposition with balloon injury compared with no injury. This is similar to observations made in comparisons of injury and injury with aspirin.

Periprocedural myocardial infarction can occur even in seemingly uncomplicated interventional procedures, and the incidence after stent placement is comparable to and possibly higher than that after BA.[14-16] Antiplatelet agents such as glycoprotein IIb/IIIa receptor inhibitors are effective in reducing the incidence of this complication during stent implantation.[17] Both systemic antiplatelet medication and local management of vascular injury are essential in the reduction of complications after intravascular intervention. Because the LLS technique can be used to continuously detect platelet microaggregates that reflect the severity of the prothrombotic vascular activation of platelets, it may be used as a technique to test drug effect of inhibition or induction of platelet aggregation. These could include additional mechanical (eg, additional stent or longer balloon inflation) or pharmacological (eg, IIb/IIIa receptor inhibitor) intervention to remedy local prothrombotic activity.

The main limitation of the LLS method is the fact that the presence of RBCs in the path of the optical beam can cause interference with particle-size distribution. In this experiment, the arteries were perfused with PRP. According to Turitto and Baumgartner et al,[18-20] the presence of RBCs in PRP enhances the intensity of platelet activity. This effect was linearly correlated with the numner of RBCs present. At this time the LLS method is not suitable for in vivo detection of platelet aggregation in whole blood, but it is suitable for the evaluation of the effects of antiplatelet agents on aggregation in a perfusing solution with a low number of RBCs. Given that many antiplatelet agents are used clinically in combination without a clear knowledge of potential additive effects, the evaluation of antiplatelet agents in our LLS-based system could be very useful. Also, we demonstrated that an RBC content of up to 6×10^6/mL did not alter the optical pattern significantly. Future studies using more RBCs may be used to evaluate the effects on various antiplatelet agents.

We thank Dr Joel Eisenberg for reviewing the manuscript. Flow cytometry was carried out at the Michigan State University Flow Cytometry Facility. We also thank Ewa Danielewicz for technical support in SEM at the Center for Advanced Microscopy of Michigan State University.

REFERENCES

1. Hubbell JA, Pohl PI , Wagner WR. The use of laser-light scattering and controlled shear in platelet aggregometry. Thromb Haemost 1991;65:601-7.
2. Eto K, Takeshita S, Ochiai M, Ozaki Y, Sato T, Isshiki T. Platelet aggregation in acute coronary syndromes: use of a new aggregometer with laser light scattering to assess platelet aggregability. Cardiovasc Res 1998;40:223-9.
3. Poullis M. A quick simple method of determining platelet aggregability following glycoprotein IIb/IIIa receptor inhibitor administration. Cardiology 1999;91:156-60.
4. Kawahito K, Kobayashi E, Iwasa H, Misawa Y, Fuse K. Platelet aggregation during cardiopulmonary bypass evaluated by a laser-light scattering method. Ann Thorac Surg 1999;67:79-84.
5. Prieto AR, Ma H, Huang R, Khan G, Schwartz KA, Hage-Korban EE, et al. Thrombostatin, a bradykinin metabolite, reduces platelet activation in a model of arterial wall injury. Cardio Res 2002;53:984-92.
6. Born GVR. Aggregation of blood platelets by adenosine diphosphate and its reversal. Nature 1962;194:927-9.
7. Cardinal DC, Flower RJ. The electronic aggregometer: a novel device for assessing platelet behavior in blood. J Pharmacol Methods 1980;3:135-58.
8. Ozaki Y, Satoh K, Yatomi Y, Yamamoto T, Shirasawa Y, Kume S. Detection of platelet aggregates with a particle counting method using light scattering. Anal Biochem 1994;218:284-94.
9. Satoh K, Ozaki Y, Qi R, Yang L, Asazuma N, Yatomi Y, et al. Factors that affect the size of platelet aggregates in epinephrine-induced activation: a study using the particle counting method based upon light scattering. Thromb Res 1996;81:515-23.
10. Tohgi H, Takahashi H, Watanabe K, Kuki H, Shirasawa Y. Development of large platelet aggregates from small aggregates as determined by laser-light scattering: effects of aggregant concentration and antiplatelet medication. Thromb Haemost 1996; 75:838-43.
11. Dehmer GJ, Nichols T, Bode AP, Liles D, Sigman J, Li S, et al. Assessment of platelet activation by coronary sinus blood sampling during balloon angioplasty and directional coronary atherectomy. Am J Cardiol 1997;80:871-7.
12. Scharf RE, Tomer A, Marzec UM, Teirstein PS, Ruggeri ZM, Harker LA. Activation of platelets in blood perfusing angioplasty-damaged coronary arteries: flow cytometric detection. Atheroscler Thromb 1992;12:1475-87.
13. Michelson AD, Barnard MR, Krueger LA, Valeri CR, Furman MI. Circulating monocyte-platelet aggregates are a more sensitive marker of in vivo platelet activation than platelet surface P-selectin: studies in baboons, human coronary intervention, and human acute myocardial infarction. Circulation 2001;104:1533-7.
14. Morishima I, Sone T, Mokumo S, Taga S, Shimauchi A, Oki Y, et al. Clinical significance of no-reflow phenomenon observed on angiography after successful treatment of acute myocardial infarction with percutaneous transluminal coronary angioplasty. Am Heart J 1995;130:239-43.
15. Abbo KM, Dooris M, Glazier S, O'Neill WW, Byrd D, Grines CL, et al. Features and outcome of no-reflow after percutaneous coronary intervention. Am J Cardiol 1995;75:778-82.
16. Adgey AA, Mathew TP, Harbinson MT. Periprocedural creatine kinase-MB elevations: long-term impact and clinical implications. Clin Cardiol 1999;22:257-65.
17. The Evaluation of Platelet Inhibitor for Stenting (EPISTENT) Investigators. Randomised placebo-controlled and balloon-angioplasty-controlled trial to assess safety of coronary stenting with use of platelet glycoprotein-IIb/IIIa blockade. Lancet 1998; 352:87-92.
18. Turitto VT, Weiss HJ. Red blood cells: their dual role in thrombus formation. Science 1980;207:541-3.
19. Turitto VT, Baumgartner HR. Platelet interaction with subendothelium in flowing rabbit blood: effect of blood shear rate. Microvasc Res 1979;17:38-54.
20. Baumgartner HR, Turitto V, Weiss HJ. Effect of shear rate on platelet interaction with subendothelium in citrated and native blood. II. Relationships among platelet adhesion, thrombus dimensions, and fibrin formation. J Lab Clin Med 1980;95:208-21.
21. Bohren CF, Huffman DR. Absorption and scattering of light by small particles. New York: John Wiley & Sons, 1998.
22. Wiscombe WJ. Mie scattering calculations: advances in technique and fast, vector-speed computer codes. Boulder, Colo: National Center For Atmospheric Research, 1979.
23. Wiscombe WJ. Improved Mie scattering algorithms. Appl Opt 1980;19:1505-9.

APPENDIX

The physical and chemical properties of a microscale aggregate such as blood platelets can be experimentally studied with the use of Mie scattering and Raman spectroscopy. Mie scattering can determine the average radius when the refractive index of the aggregate is known.

The typical Mie-scattering measurement on liquid suspensions employs a laser beam as the light source. This laser beam is scattered in all the directions at the suspension liquid. The measurement of the relative intensity at various scattering angles reveals the average radius and the relative refractive index of the microscale particles in suspension. Mie theorem describes the light scattering from homogeneous spheres. The authors argue that the Mie theorem is adequate for our work of measuring the degree of blood-platelet aggregation because the blood platelet aggregates roughly into spherical shapes.

A laser beam is a high-intensity coherent varying electromagnetic wave. When this electromagnetic wave is applied to a material, it interacts with the nuclei and electrons strongly, stimulating oscillations of nuclei and electrons in the material. The oscillating electrons and nuclei reradiate electromagnetic waves in all directions, resulting in scattered light. The theory on the scattering of electromagnetic wave by spherical objects was first developed by Mie in the early 1900s and is called Mie's scattering.[21]

A static electromagnetic wave has the form:

$$\nabla^2 \mathrm{H} + \frac{n^2\omega^2}{c^2}\mathrm{H} = 0 \quad \nabla^2 \mathrm{E} + \frac{n^2\omega^2}{c^2}\mathrm{E} = 0$$

$$\nabla \times \mathrm{H} = -i\frac{\omega\varepsilon}{c}\mathrm{E} \quad \nabla \times \mathrm{E} = i\frac{\omega\mu}{c}\mathrm{H}$$

where $n = \sqrt{\varepsilon\mu}$ is the refractive index of the material, H is the magnetic field, E is the electric field, and ω is the frequency of the electromagnetic wave.

The incident electromagnetic field of the laser is taken as a plane wave. When this electromagnetic wave is applied to a spherical homogenous material, it is both reflected and refracted. The electromagnetic field everywhere is the summa-

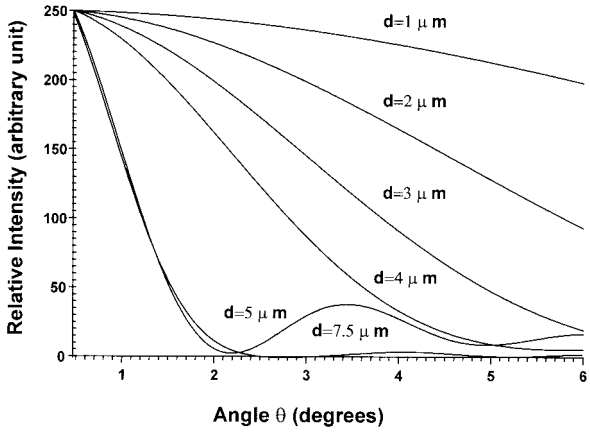

Fig 9. LLS for spherical particles with refractive index of 1.05 and diameters ranging from 1 to 7.5 μm. These curves were derived by way of the Mie theory with MIEV software.[22,23] The curves demonstrate that smaller particles have a greater effect on scattering light at wider angles.

tion of the incident, reflected, and refracted fields. The electromagnetic field should satisfy the above wave equation everywhere. In the infinity limit, the total electromagnetic fields should be a plane wave. The electromagnetic field should satisfy the boundary condition at the surface of the sphere. From the above considerations, we can solve the scattered electromagnetic wave equation as:

$$\mathrm{E}_s = E_0 \sum_{k=1}^{\infty} i^k \frac{2k+1}{k(k+1)} (i a_k \mathrm{N}_{elk}^{(3)} - b_k \mathrm{M}_{olk}^{(3)})$$

$$\mathrm{H}_s = \frac{1}{c}\sqrt{\frac{\varepsilon_{solvent}}{\mu_{solvent}}} E_0 \sum_{k=1}^{\infty} i^k \frac{2k+1}{k(k+1)} (a_k \mathrm{M}_{elk}^{(3)} + i b_k \mathrm{N}_{olk}^{(3)})$$

with

$$a_k = \frac{\mu_{solvent} m^2 j_k(mx)[x j_k(x)] - \mu_{sphere} j_k(x)[mx j_k(mx)]}{\mu_{solvent} m^2 j_k(mx)[x h_k^{(1)}(x)] - \mu_{sphere} h_k^{(1)}(x)[mx j_k(mx)]}$$

$$b_k = \frac{\mu_{sphere} j_k(mx)[x j_k(x)] - \mu_{solvent} j_k(x)[mx j_k(mx)]}{\mu_{sphere} j_k(mx)[x h_k^{(1)}(x)] - \mu_{solvent} h_k^{(1)}(x)[mx j_k(mx)]}$$

where the relative refractive index is the ratio of refractive index of the sphere over that of the solvent:

$$m = \frac{n_{sphere}}{n_{solvent}}$$

The intensity of the scattered light, which is the Pointing vector is defined as:

$$\mathrm{S} = \frac{c}{4\pi} \mathrm{E}_s \times \mathrm{H}_s$$

Both the electric and magnetic fields are polynomial functions of the scattering angle θ. The intensity also depends on the relative refractive index and the radius of the sphere. The graph demonstrates the intensity as a function of scattering angle with a fixed relative refractive index of 1.05 at various sphere radii (Fig 9).[22,23]